Author's personal copy

Materials Letters 82 (2012) 112–115

Contents lists available at SciVerse ScienceDirect

Materials Letters

journal homepage: www.elsevier.com/locate/matlet

Facile synthesis of ultra-small Bi_2Te_3 nanoparticles, nanorods and nanoplates and their morphology-dependent Raman spectroscopy

Liangliang Chen, Qing Zhao, Xiulin Ruan *

School of Mechanical Engineering and Birck Nanotechnology Center, Purdue University, West Lafayette, IN 47907, USA

ARTICLE INFO

Article history:
Received 16 March 2012
Accepted 26 April 2012
Available online 11 May 2012

Keywords:
Bi2Te3
Nanorod
Nanoparticle
Nanoplate
Raman
TEM

ABSTRACT

High-crystalline 0D, 1D and 2D ultra-small Bi_2Te_3 nanocrystals were synthesized using the pyrolysis of organometallic compound method. The Bi_2Te_3 nanocrystals was studied with transmission electron microscopy (TEM). Samples synthesized at 35 °C possessed a dominant morphology of 0D nanoparticles or 1D nanorods, while samples synthesized at temperatures higher than 75 °C possessed a dominant morphology of 2D nanoplates. Phonon vibrations were investigated by Raman spectroscopy. The 2D nanoplates showed similar Raman features as few-quintuple-thick Bi_2Te_3 layers, while the 0D and 1D nanostructures showed a blue-shifted A_{1g}^2 mode and a much stronger A_{1u} mode. This is the first report regarding the morphology effect on the Raman-active phonon modes of Bi_2Te_3 nanocrystals.

© 2012 Elsevier B.V. All rights reserved.

1. Introduction

Bismuth telluride based alloys have received extensive attention by virtue of their excellent TE performance at room temperature. Bulk Bi_2Te_3-based alloys possess a ZT value close to 1 [1]. However, in order for TE power generation to become competitive to other power generation approaches, a ZT value of 4 is required [2].

Theoretical studies showed that making bulk TE materials into nanostructures could enhance their performance by decreasing their phonon thermal conductivity. Hicks et al. showed that the ZT value of Bi_2Te_3 quantum well might be 9 times higher than the bulk value [3] and the ZT value of 1D Bi_2Te_3 nanowire could be increased to ~14 from the bulk value [4].

Despite the progress in the synthesis of Bi_2Te_3 nanocrystals [5–8], the synthesis of pure-phase Bi_2Te_3 nanoparticles smaller than 10 nm still remains a challenge due to the high reactivity between bismuth and tellurium salts. To summarize, Bi_2Te_3 nanoparticles can be synthesized via methods like co-precipitation [9], reverse micelle [10], micro-emulsion [11], reduction of metal-organo complexes [12], and hydrothermal (solvothermal) method [8]. Due to the application of high pressure, hydrothermal (solvothermal) approaches normally result in oversized Bi_2Te_3 nanocrystals [8]. Purkayastha et al. [11] developed a micro-emulsion method to synthesize Bi_2Te_3 nanoparticles of 5 nm, however the XRD results showed the existence of sulfur-related impurities. Scheele et al. [12] used a two-step reduction method to produce nanoparticles of 7 nm, but there was still a trace of impurities.

Raman spectroscopy has been used to detect the lattice vibration of Bi_2Te_3 materials. With Raman spectroscopy, the influence of thickness in few-quintuple Bi_2Te_3 layers and chemical stoichiometry in Bi_2Te_3 films has been studied [5–7,13]. To our best knowledge, no work has been done to study the phonon modes in Bi_2Te_3 nanorods and small Bi_2Te_3 nanoparticles whose sizes are within the strong quantum confinement region.

In this work, using pyrolysis of organometallic compounds, high-crystalline, pure Bi_2Te_3 nanoparticles as small as 2 nm were synthesized. Furthermore, Bi_2Te_3 nanocrystals of various morphologies were also synthesized. The morphology effect on the phonon vibrations in Bi_2Te_3 nanocrystals was then studied.

2. Experimental details

All chemical reagents, unless stated otherwise, were purchased from Alfa Aesar. For synthesis, a mixture of 1.82 mmol tellurium powder and 3 ml tri-n-octylphosphine was loaded into a flask and then heated up to 250 °C. The solution turned clear in 5 min and was immediately removed from the heater and transferred into a syringe for injection after it cooled down. A mixture of 1.22 mmol bismuth acetate, 20 ml oleic acid (TCI America), and 20 ml octadecene was loaded into a flask and then heated to different temperatures and kept there for 10 min. After the solution turned clear, the tellurium precursor was quickly injected (<0.5 s) with vigorous stirring. After injection, the temperature of the solution dropped by 5° and was kept at that temperature until the reaction was quenched. The as-prepared nanocrystals were precipitated by adding a mixture of

* Corresponding author. Tel.: +1 765 494 5721; fax: +1 765 494 0539.
E-mail address: ruan@purdue.edu (X. Ruan).

0167-577X/$ – see front matter © 2012 Elsevier B.V. All rights reserved.
doi:10.1016/j.matlet.2012.04.135

Author's personal copy

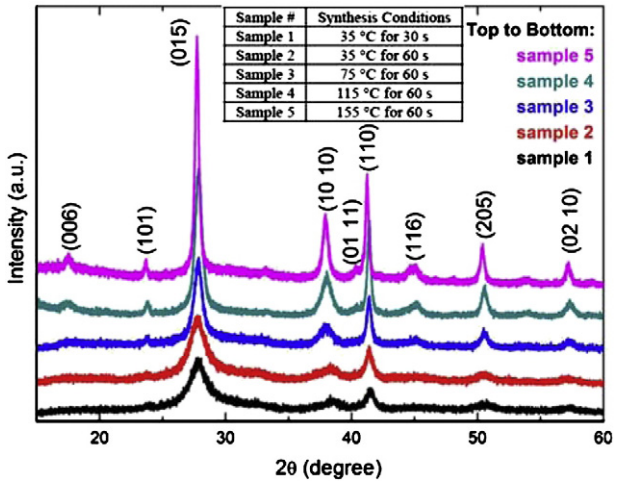

Fig. 1. X-ray diffraction patterns and synthesis conditions (inset) of Bi2Te3 samples.

ethanol and acetone to the solution and then washed by repeating the dispersion/precipitation cycle three times. The synthesis detail of each sample is shown in Fig. 1.

For characterization, the washed samples were either dissolved in hexanes or deposited on glass substrates. X-ray diffraction patterns were recorded on Bruker D8 X-ray Diffractometer. TEM and HRTEM images were taken on Titan Field-Emission TEM with an accelerating voltage of 300 kV. Raman spectra were recorded at room temperature on Renishaw Invia Raman Microscope. The 633 nm excitation laser had a spot size of 5 μm and a power of 0.5 mW.

3. Results and discussions

XRD patterns are shown in Fig. 1. All the patterns match the record of rhombohedral-structured Bi_2Te_3 (JCPDS 82–0358). No unidentified peaks exist, indicating that the samples are impurity-free.

Representative TEM images are shown in Fig. 2. Fig. 2a and b is taken at different locations of Sample 1, made at the lowest reaction temperature (35 °C) that can yield Bi_2Te_3. The average size of nanoparticles in Sample 1 is 3 ± 1 nm, much smaller than nanoparticles made by other groups. The inset of Fig. 2a is the high-resolution TEM image of a single nanoparticle in Sample 1. Despite the existence of some lattice faults, the existence of periodical atomic arrangement confirms the high crystallinity of the nanoparticle. Although no obvious agglomeration of nanoparticles is observed and the dominant morphology is 0D nanoparticle in Sample 1, some nanoparticles are seen to self-arrange into line shapes, shown in Fig. 2b, indicating the tendency of nanoparticles growing into nanorods.

Fig. 2c shows the morphology of Sample 2, produced with a longer reaction time compared with Sample 1. Bi_2Te_3 nanorods have formed in Sample 2, matching the tendency of nanoparticles self-arranging into the line shape seen in Sample 1. The diameters of nanorods in Sample 2 match the diameters of nanoparticles in Sample 1. Although in Sample 2 some nanoparticles have grown into quasi-2D nanoflakes, the dominant morphology is 0D nanoparticle and 1D nanowire.

Fig. 2d shows the morphology of Sample 3, made at a higher temperature compared with Sample 2. Compared with Sample 2, the growth of quasi-2D nanoflakes in Sample 3 has been significantly boosted, changing the dominant morphology from 0D and 1D nanocrystals in Sample 2 to 2D nanoplates in Sample 3.

Fig. 2e and f shows the morphologies of Samples 4 and 5 respectively, both made at higher temperatures compared with Sample 3. It is seen that further increase in reaction temperature leads to no significant morphology change but improvement in the crystallinity. Although both 1D nanorods and 2D nanoplates have been observed to grow larger, the dominant morphology is still 2D nanoplates in both Samples 4 and 5. The murky image of nanoplates in Sample 4 can be traced back to the partially crystallized parts and hence a relatively low local crystallinity, while Fig. 2f shows that the crystallinity has been improved in Sample 5, which can be attributed to the increased reaction temperature. The morphology information of each sample is summarized in Fig. 4.

Fig. 3 shows a high-magnification TEM image and its corresponding fast Fourier transform electron diffraction pattern (FFTEDP) obtained on the nanoplate in Sample 5. The uniform contrast all over the image confirms the thickness uniformity of the nanoplate. The diffraction pattern

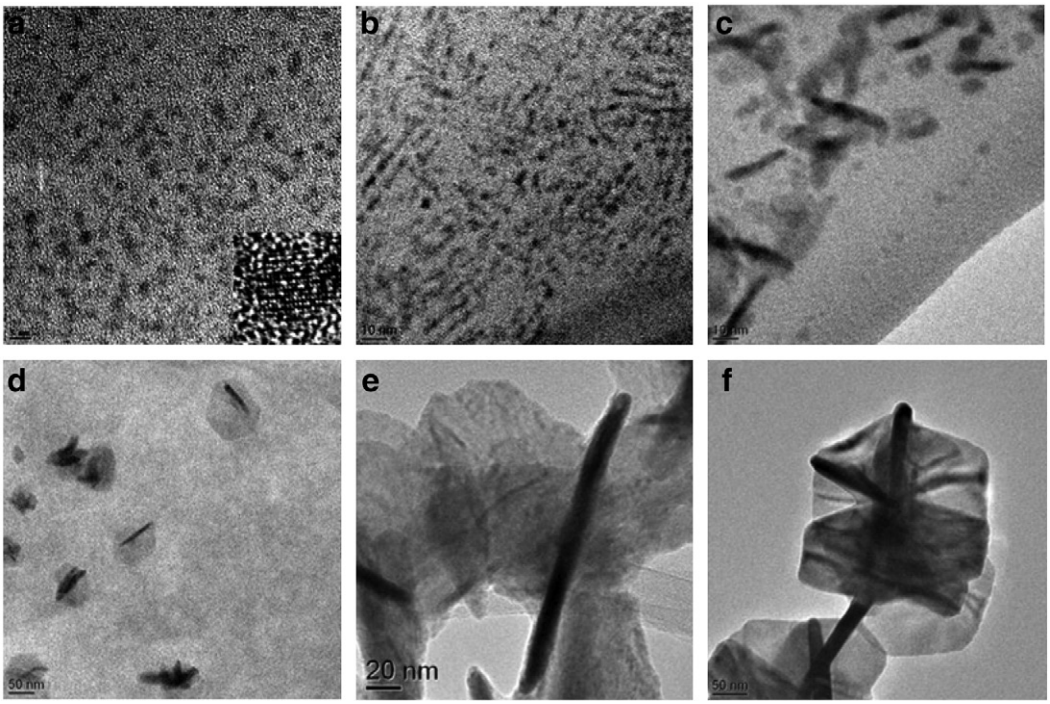

Fig. 2. Typical TEM images of Sample 1 (a and b), Sample 2 (c), Sample 3 (d), Sample 4 (e), and Sample 5 (f). HRTEM image of a single nanoparticle in Sample 1 (inset in a).

Author's personal copy

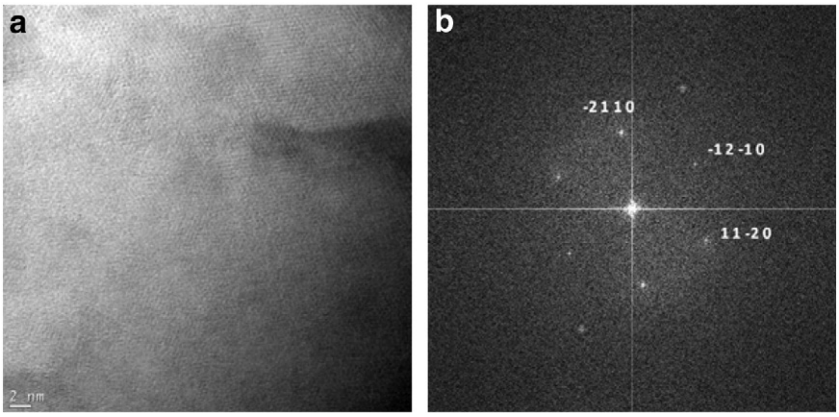

Fig. 3. High-magnification TEM image (a) and fast Fourier transform diffraction pattern (b) taken on Sample 5.

in the FFTEDP shows six-fold symmetry and can be matched with the projection of the Bi_2Te_3 reciprocal lattice in [0001] diffraction, implying both surfaces of the nanoplate are parallel to {0001} planes.

With the Bi_2Te_3 nanocrystals of various morphologies, the morphology effect on Raman features is systematically studied. Representative Raman spectra are shown in Fig. 4. All the spectra are normalized to the intensity of A_{1u} mode. Five samples show two distinct sets of Raman features. The spectra of Samples 1 and 2 are similar, while the spectra of Samples 3, 4 and 5 are similar.

In the spectra of Samples 3, 4 and 5, three vibrational modes, E_g^2, A_{1u}, and A_{1g}^2, are present, among which E_g^2 and A_{1g}^2 are Raman active and A_{1u} is forbidden in bulk Bi_2Te_3. However, Tewelderhan et al. [6,7] have shown that the A_{1u} mode shows up in 2D few-quintuple Bi_2Te_3 layers due to the symmetry breaking in atomically-thin films. Considering the dominant morphology in Samples 3, 4 and 5 is 2D nanoplate, it's reasonable that their Raman features match the record of 2D few-quintuple Bi_2Te_3 layers [6,7].

Due to symmetry breaking, A_{1u} mode becomes active not only in 2D nanostructure, but also in 0D and 1D structures. As the dimension shrinks from 2D to lower dimensions, the relative intensity of A_{1u} mode increases, which obscures the in-plane E_g^2 mode and makes it almost invisible, and the frequency of the A_{1g}^2 mode shifts from 135 cm^{-1} to 143 cm^{-1}. Although previous investigations on the blueshift of Raman modes in semiconductor nanocrystals have proposed several possible causes, like lattice contraction [14] and temperature decrease [15], the origin of the A_{1g}^2-mode blueshift from 2D structure to 0D/1D structure is not clear yet. Considering the morphology difference between 2D and 0D/1D structures, the blueshift of the mode can be induced by the shrink in the axial direction of the 0D/1D structure.

4. Conclusions

In conclusion, we have synthesized high-crystalline, impurity-free Bi_2Te_3 nanoparticles as small as 2 nm. We have also synthesized Bi_2Te_3 nanocrystals of various morphologies and systematically studied the growth of Bi_2Te_3 nanocrystals. The reaction temperature has a significant influence of the morphology of the nanocrystals. 0D/1D morphologies are dominant at low reaction temperatures, while 2D morphology becomes dominant at temperatures above 75 °C. Phonon vibrations have been studied by Raman spectroscopy. The originally Raman-inactive mode in bulk Bi_2Te_3, A_{1u}, appears in all 0D, 1D and 2D nanocrystal samples. With further shrink in dimension from 2D to 1D and 0D, the A_{1u} phonon mode is further intensified and the A_{1g}^2 mode shifts to the higher-frequency side.

Acknowledgements

This work was partially supported by the National Science Foundation (Award # CBET-0933559) and the Purdue Cooling Technologies Research Center, an NSF-Industry Cooperation Research Center. Discussions with Dr. Bhat are appreciated.

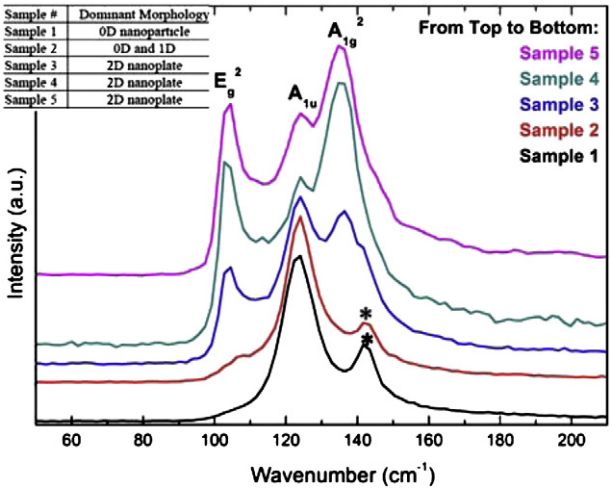

Fig. 4. Raman spectra and summary of dominant morphologies (inset) of Bi2Te3 samples.

Author's personal copy

References

[1] Rowe DM. Thermoelectrics handbook: macro to nano. illustrated ed: CRC Press, Boca Raton; 1995.
[2] Chen G, Shakouri A. Heat transfer in nanostructures for solid-state energy conversion. J Heat Trans-T Asme 2002;124:242–52.
[3] Hicks LD, Dresselhaus MS. Effect of quantum-well structures on the thermoelectric figure of merit. Phys Rev B 1993;47:12727–31.
[4] Hicks LD, Dresselhaus MS. Thermoelectric figure of merit of a one-dimensional conductor. Phys Rev B 1993;47:16631–4.
[5] Zhao Y, Hughes RW, Su Z, Zhou W, Gregory DH. One-step synthesis of bismuth telluride nanosheets of a few quintuple layers in thickness. Angew Chem Int Ed 2011;50: 10397–401.
[6] Teweldebrhan D, Goyal V, Balandin AA. Exfoliation and characterization of bismuth telluride atomic quintuples and quasi-two-dimensional crystals. Nano Lett 2010;10:1209–18.
[7] Teweldebrhan D, Goyal V, Rahman M, Balandin AA. Atomically-thin crystalline films and ribbons of bismuth telluride. Appl Phys Lett 2010;96.
[8] Zhou LN, Zhang XB, Zhao XB, Zhu TJ, Qin YQ. Influence of NaOH on the synthesis of Bi2Te3 via a low-temperature aqueous chemical method. J Mater Sci 2009;44: 3528–32.
[9] Ritter JJ. A novel synthesis of polycrystalline bismuth telluride. Inorg Chem 1994;33: 6419–20.
[10] Foos EE, Stroud RM, Berry AD. Synthesis and characterization of nanocrystalline bismuth telluride. Nano Lett 2001;1:693–5.
[11] Purkayastha A, Kim S, Gandhi DD, Ganesan PG, Borca-Tasciuc T, Ramanath G. Molecularly protected bismuth telluride nanoparticles: microemulsion synthesis and thermoelectric transport properties. Adv Mater 2006;18:2958-+.
[12] Scheele M, Oeschler N, Meier K, Kornowski A, Klinke C, Weller H. Synthesis and thermoelectric characterization of Bi(2)Te(3) nanoparticles. Adv Funct Mater 2009;19:3476–83.
[13] Russo V, Bailini A, Zamboni M, Passoni M, Conti C, Casari CS, et al. Raman spectroscopy of Bi–Te thin films. J Raman Spectrosc 2008;39:205–10.
[14] Zhang JY, Wang XY, Xiao M, Qu L, Peng X. Lattice contraction in free-standing CdSe nanocrystals. Appl Phys Lett 2002;81:2076–8.
[15] Tanaka A, Onari S, Arai T. Raman-scattering from CdSe microcrystals embedded in a germanate glass matrix. Phys Rev B 1992;45:6587–92.